

RoMo: A Large-Scale, Richly Organized Dataset and Semantic Taxonomy for Human Motion Generation

Jiahao Zhang^{1,2} Joseph Liu² Young-Yoon Lee² Seonghyeon Moon²
 Victor Zordan² Guy Tevet³ C. Karen Liu³ Stephen Gould¹
 Oren Jacob² Haomiao Jiang² Mubbasir Kapadia^{2,4} Yizhak Ben-Shabat²
¹Australian National University ²Roblox ³Stanford University ⁴Rutgers University

¹{jiaho.zhang, stephen.gould}@anu.edu.au

²{josephliu, ylee, smoon, vbzordan, haomiaojiang, ojacob, mkapadia, ibenshabat}@roblox.com

³{guytevet, karenliu}@cs.stanford.edu

<https://davidzhang73.github.io/romo-website>

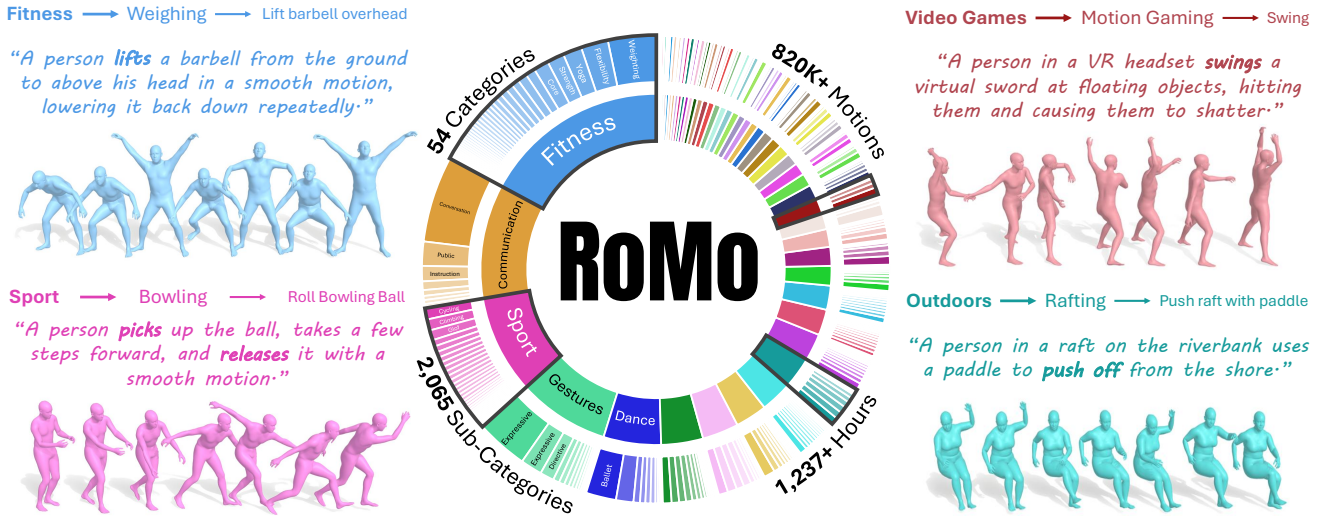


Figure 1. We present **RoMo**, a large hierarchical dataset of 820K in-the-wild 3D human motions with detailed text captions organized into a three-level taxonomy (Category → Subcategory → Atomic-action), and annotated with text-rich prompts. The pie chart shows the distribution of categories and subcategories, while four examples illustrate diverse motions.

Abstract

Success in generative modeling across language, image, and video demonstrates that large, well-curated datasets are the key driver for building capable models. 3D Human motion, however, has lagged behind, constrained by an unsatisfying choice between small, high-fidelity motion capture datasets and large-scale in-the-wild collections dominated by static or low-quality sequences.

We introduce **RoMo**, a rich, large-scale, carefully curated dataset of in-the-wild human motions that resolves these tradeoffs. To ensure quality, we introduce a taxonomy-aware filtering pipeline that aggressively removes static

and artifact-prone sequences. Every sequence is annotated with detailed captions and organized by a novel three-level semantic taxonomy. This hierarchical structure enables fine-grained, per-category evaluation, that reveals model strengths and weaknesses obscured by global metrics.

We demonstrate that models trained on RoMo achieve state-of-the-art fidelity and diversity while gaining a superior understanding of complex, subtle text prompts. Finally, we release the Motion Toolbox to standardize metrics, data conversion, and visualization, establishing a foundation for reproducible and interpretable motion generation research.

1. Introduction

3D human motion generation has advanced rapidly with the rise of diffusion [25, 79] and GPT [21, 66] models, enabling high-fidelity synthesis and a wide range of controllable behaviors. At the foundation of this progress lies the dataset. Learning from the scaling success in language [19], image [37], and video [89] generation, the field has attempted to move beyond small, high-fidelity motion capture collections by extracting poses from in-the-wild videos. In practice, however, these pioneering large-scale efforts suffer from minimal curation, resulting in datasets dominated by static, noisy, or artifact-prone sequences. This has led to an unsatisfying choice: train on small, clean datasets that no longer challenge modern models, or on massive but unreliable collections that bias models toward static, low-quality motion. This tradeoff limits progress, as neither option provides the reliable, fine-grained data needed to train or evaluate truly compositional human motion.

To address these challenges, we introduce **RoMo**, a large-scale collection of in-the-wild 3D human motion paired with rich textual and categorical annotations. The dataset is built on three pillars: *scale*, *curation*, and a *coarse-to-fine taxonomy*. Together, these components create a foundation for reliable training and transparent evaluation in motion generation.

First, we gather an unprecedented volume of videos depicting diverse human activities from multiple online sources. Each clip is processed with a SOTA pose estimation model, GVHMR [71], to extract accurate 3D motion sequences. To enrich the semantic context, we employ vision-language models to generate multiple detailed captions per clip, capturing both the action and its environment.

Second, we place strong emphasis on curation. Instead of releasing raw, noisy data, we apply a multi-stage filtering pipeline guided by quantitative motion metrics to remove static, incomplete, or artifact-prone samples. The filtering process is adaptive: for example, motions in the “fishing” category are expected to be more subtle than those in “acrobatics” and the threshold is adjusted accordingly to retain only realistic, category-consistent sequences.

Finally, we propose a new hierarchical taxonomy for human motion, organizing each sequence into categories, sub-categories, and atomic actions. This taxonomy introduces a structured way to analyze and evaluate motion generation models. It enables researchers to assess performance per category, revealing specific strengths, weaknesses, and blind spots, while also ensuring balanced coverage of the human motion space and mitigating dataset bias.

To further advance reproducibility and accessibility, we release the **Motion Toolbox**, a unified framework for data conversion, standardized evaluation metrics, and browser-based visualization. Together, these contributions establish a new foundation for large-scale, transparent, and semanti-

cally grounded research in generative human motion.

We demonstrate that RoMo drives substantial gains in fidelity, diversity, and prompt understanding. Contemporary motion generation models [16, 79] trained on our benchmark respond to subtle textual nuances and generalize to scenarios out of distribution in prior datasets. Leveraging our taxonomy, we perform the first per-category evaluation of generative models, revealing that state-of-the-art models, while excelling at common actions, fail on fine-grained categories with subtle interactions. This union of data scale, motion quality, rich text prompts, and taxonomy structured evaluation surfaces research gaps that previous datasets could not reveal and lays the groundwork for the next stage of human motion generation.

The main contributions of this paper are:

- **RoMo:** A new large-scale, in-the-wild motion dataset (1237h, 820K clips) with five rich text captions per clip and high-quality, filtered motion.
- **A Novel Curation & Taxonomy Framework:** We introduce a hierarchical semantic taxonomy (54 categories, 2,065 subcategories) and a *taxonomy-aware adaptive filtering pipeline* that uses it to ensure high motion quality and diversity.
- **The Motion Toolbox:** An open-source library for standardized evaluation, data conversion, and browser-based visualization to accelerate reproducible research.

2. Related Works

Table 1 presents a comparison of publicly available human motion datasets, from motion capture and video sources.

Human Motion Generation. In recent years, human motion generation has made remarkable progress, driven by the adaptation of modern machine learning paradigms. AC-TOR [60] and MotionCLIP [78] introduced a transformer-based auto-encoder for effective motion synthesis [88]. MDM [79] advanced the field by applying diffusion models [25], enabling diverse and high-fidelity text-to-motion generation. Building on this direction, DiP [80] and CAMDM [13] brought diffusion to real-time performance. In parallel, inspired by the success of GPT [66] models in language generation, several works [21, 31, 96] demonstrated that human motion can be tokenized and generated as a sequence of discrete motion tokens [87]. MoMask [22] introduced a residual quantization to enhance fidelity.

These generative approaches have been successfully applied to a wide range of animation tasks, including text-to-motion [31, 54], music-driven motion [3, 15, 38, 74, 84], motion stylization [68, 99], multi-person [43, 70], and human-object interaction [40, 41, 59, 62, 67, 97]. Alongside these advances, a variety of techniques for fine-grained control have emerged, leveraging diffusion guidance [34], inpainting [14, 70], noise optimization [35], and attention injections [65]. However, this entire line of research mostly

Table 1. Comparison of RoMo with existing publicly available 3D motion datasets with free-form text annotations. RoMo is the first to integrate both a large-scale hierarchical semantic taxonomy and a massive-scale dataset, featuring 820K core clips (1237.8 hours). For clarity, in the table: ‘Text diversity’ refers to the number of captions per motion sequence. ‘Clip Number’ reports both the core set (new motion sequences proposed in that work) and the total clips.

Dataset	Hierarchical Semantic Taxonomy	Category Sub-category	Clip Number Core (Total)	Hour	Text Diversity	Source	Scene		
							Indoor	Outdoor	RGB
KIT-ML [63]	✗	-	3.9K (3.9K)	11.2 (11.2)	1-3	MoCap	✓	✗	✗
BABEL [64]	✓	8 / 260	13K (13K)	43.5 (43.5)	1	MoCap	✓	✗	✗
HumanML3D [20]	✗	-	0 (15K)	0 (28.6)	1-3	MoCap	✓	✗	✗
SnapMoGen [29]	✗	-	20K (20K)	43.7 (43.7)	6	MoCap	✓	✗	✗
Motion-X [44]	✗	-	48.6K (81.1K)	86 (144.2)	1	Video+MoCap	✓	✗	✗
Motion-X++ [98]	✗	-	39.4K (120.5K)	59 (180.9)	1	Video+MoCap	✓	✗	✗
MotionMillion [16]	✗	-	560K (2M)	726.5 (2000)	>20	Video	✓	✓	✓
RoMo (ours)	✓	54 / 2065	820K (2.58M)	1237.8 (3023)	5	Video	✓	✓	✓

relies on a small set of motion capture datasets. This constrains these powerful models, limiting their ability to learn the diversity and nuance of complex, in-the-wild human motion—a gap we directly address with RoMo.

Motion Capture Collections. Motion capture (mocap) has long served as the gold standard for recording 3D human motion in character animation. Using wearable sensors [27], optical markers [30, 52], or calibrated multi-view systems [33], mocap provides highly accurate reconstructions of body movement. AMASS [50] unified a collection of academic mocap datasets [1, 2, 4, 7, 8, 10, 12, 17, 18, 23, 26, 36, 42, 47, 48, 51, 53, 57, 73, 75, 81–83, 86] by converting them into a consistent SMPL [46] representation, establishing a common format for research. BABEL [64] extended this effort with basic textual annotations, while HumanML3D [20] curated a refined subset of AMASS with detailed textual descriptions, making it the most widely used dataset for text-to-motion generation. Additional collections such as AIST++ [85] captured around five hours of dance motion paired with music, while GRAB [76], OMOMO [40], and HUMOTO [49] introduced object interactions, hand articulation, and multi-person motions, each annotated with textual action descriptions. However, mocap remains an expensive and time-consuming process, and even the combined output of academic collaborations around the globe amounts to fewer than 20K motions [50]. This small scale, in stark contrast to the 400M images in LAION [69], makes it impossible for MoCap-based datasets to capture the ‘long tail’ of diverse human activities that RoMo is designed to represent.

Motions from Videos In-the-wild. Recent progress in 3D human and camera pose estimation [71, 72, 94] has opened the door to extracting motion directly from monocular in-the-wild videos. This raises the question of whether it can be leveraged to break the scale limitations of motion capture. Motion-X [44, 98] and MotionMillion [16] took steps in this direction, releasing large datasets with up to a million motion sequences. Motionlib [91] also curated a

large-scale dataset, but as it has not been publicly released, it is omitted from our comparative analysis. Despite the scale of these collections, data quality remains a significant issue, as pose estimation still suffers from significant errors: inaccurate camera reconstruction can cause characters to float, temporal inconsistencies lead to jitter, and regression noise often produces anatomically implausible poses. Moreover, many collected clips are static or lack meaningful motion. As a result, these large-scale datasets, while impressive in size, often include numerous artifacts and imbalanced motion categories, underscoring the need for stronger filtering and structured organization mechanisms. This underscores the critical need for stronger filtering and structured organization. RoMo is the first dataset designed to solve both problems: our taxonomy-aware adaptive filtering pipeline addresses the quality issue, while our hierarchical taxonomy solves the lack of structured organization.

Human Motion Evaluation. Many works have proposed objective measures for motion quality, such as foot skating [34, 67, 80, 95], floating [80, 95], jitter (jerk) [5, 16, 55, 71], ground [67, 95] or self-penetration [56], and root orientation change [16], yet each study defines its metrics slightly differently, leaving no clear consensus. HumanML3D [20] established a standard for evaluating generated motion distributions by introducing neural evaluators that embed text and motion in a shared latent space to compute FID [24] and prompt adherence. SnapMoGen [29] later refined these evaluators. Our Motion Toolbox (Sec. 5) is designed to provide a single, open-source, and verified standard implementation of these key metrics.

3. Taxonomy-aware Data Pipeline

We present our fully automated, taxonomy-aware data pipeline in Fig. 2. This system extracts diverse human motions from broad web video corpora while preserving semantic coverage and motion quality.

RoMo stands on two strong foundations: a hierarchical

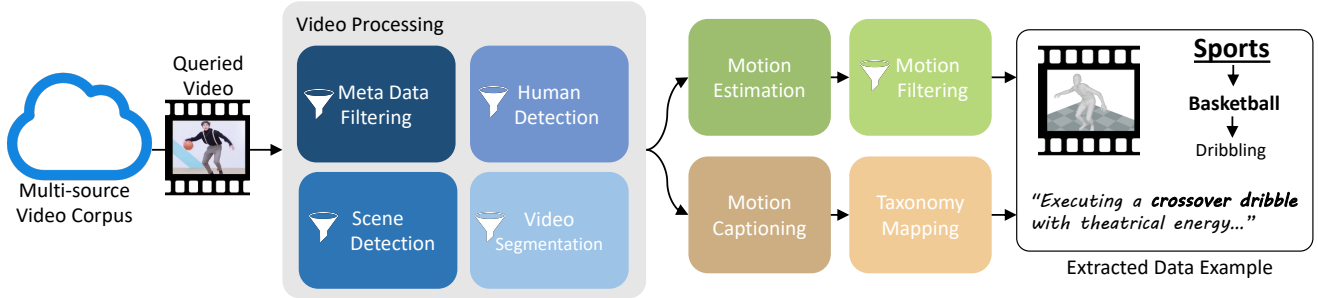


Figure 2. **Data Pipeline.** RoMo is extracted from a large web video corpus. We query human motion videos, filter single-human scenes, and segment them into atomic actions. We then apply a 3D camera and pose estimation, remove low-quality motions, and caption and categorize the results using our hierarchical taxonomy. Overall, the pipeline performs uncompromising large-scale filtering that processes 125K hours of raw footage and distills 1% into high-quality, well-annotated motions.

taxonomy of the human motion action space (Sec. 3.1) and a multi-source video corpus (Sec. 3.2). The taxonomy is a hierarchical protocol that spans the human motion manifold and organizes it into categories, subcategories, and atomic actions, providing the structural backbone of the dataset. The video corpus combines large-scale web queries with public datasets, yielding a diverse and massive pool of candidate clips that cover a wide spectrum of everyday and specialized motions.

The video processing module (Sec. 3.3) filters the queried videos based on their metadata, splits them into scenes, identifies scenes containing a single moving person, and then segments each scene into atomic action candidates. The filtered clips undergo 3D body and camera motion estimation (Sec. 3.4), followed by evaluation and filtering metrics that remove static or corrupted reconstructions (Sec. 3.5). In parallel, a vision-language model then generates descriptions of the human motion, using the visual clues in the surrounding video context to refine and disambiguate the motion phrasing, and a taxonomy-mapping stage assigns each segment to its category, subcategory, and atomic action.

Overall, the system applies aggressive filtering at a massive scale (Fig. 3), processing 125K hours (~ 14 years) of human motion videos and distilling only about one percent into 3D motion sequences of uncompromising quality with taxonomy-aligned annotations.

3.1. Motion Taxonomy

We introduce a three-level motion taxonomy to ensure broad coverage of human activities and to support evaluation at both coarse and fine semantic resolutions. The initial structure draws on action recognition literature [6, 9, 77] and was expanded to cover the diversity observed in large web corpora. This design enables hierarchical analysis. For example, if a generative model struggles with the *gestures* category, the taxonomy allows drilling down to specific ges-

ture types to identify failure modes.

The taxonomy contains three layers (Category \rightarrow Subcategory \rightarrow Atomic-action). **Categories** capture broad motion themes such as *Sports*, *Daily Activities*, and *Professions*. **Subcategories** form compact semantic groups expressed as noun phrases, for example *Table Tennis* or *Cleaning Activities*. **Atomic-actions** are short present-tense verb phrases that may include objects or body parts but avoid modifiers and punctuation, for instance *Swing racket* or *Climb stairs*. These units span only a few seconds and serve as the basis for segmentation, search, and captioning.

We construct the taxonomy with a hybrid approach. High-level categories were defined through a top-down review of major action and video datasets [6, 9, 39, 45, 58, 77, 90]. Then, 2,897 subcategories and 28,874 atomic actions were expanded through LLM-assisted term discovery, followed by human curation to refine phrasing and merge duplicates. The final structure contains 54 categories, 2,065 subcategories, and 28,874 of atomic actions. A full listing appears in the supplemental material.

3.2. Taxonomy-based Video Queries

The taxonomy structure serves as the basis for querying the video corpus looking for human motion videos: given a Category–Subcategory pair together with its Atomic Action vocabulary, an LLM synthesizes N diverse search queries that cover synonyms, salient objects, and contexts; each query retrieves up to M candidate videos from online platforms, yielding as many as $N \times M$ candidates per Subcategory after de-duplication via URL hashing and perceptual video fingerprints. We further incorporate publicly available video datasets [11, 39, 45, 90] and unify them to our taxonomy post-hoc: free-form labels or titles are first converted to normalized textual descriptions and then mapped to atomic-actions with a retrieval-augmented LLM remapper constrained by MCP (synonym tables, type checks, and rationale logging).

3.3. Video Processing and Filtering

Metadata Filtering. We first observe that a large fraction of queried videos can be discarded using metadata alone. We first remove clips that are too short or have a frame rate below 24 FPS. An LLM then reads the remaining metadata (mainly tags and descriptions) and assigns confidence scores in the range $[0, 1]$ to four criteria: (1) the description refers to a human action, (2) the action involves a single person, (3) the full body is expected to be visible, and (4) the content is not AI generated. Videos that fall below the threshold on any criterion are filtered out.

Scene Detection. To ensure each candidate clip contains exactly one visible human performing an analyzable motion, we follow MotionMillion [16] by first applying PySceneDetect to remove transitions and discontinuous segments. In addition, our method further eliminates near-static sequences based on inter-frame differences.

Single-human Detection. We then detect humans with YOLOv8 [32] and retain clips in which a single human is present in a large fraction of frames and occupies a reasonable portion of the image; extreme close-ups and tiny subjects are discarded. Finally, we estimate 2D poses with ViT-Pose [92] and reject clips with frequent truncation or low in-frame joint ratios, thereby improving downstream motion recovery robustness. The resulting clips range from seconds to minutes and are visually continuous, each dominated by a single performer.

Temporal Semantic Segmentation. A key limitation of prior large-scale motion datasets is their use of fixed-length slicing or hard duration caps, which often breaks clips at points that do not correspond to meaningful actions. MotionMillion [16] for example, inherit this issue since their segmentation is not aligned to semantic units. To address this, we perform *semantic* temporal segmentation using a state-of-the-art multimodal VLM (Qwen3-VL [93]). For each cleaned clip, the model receives the relevant taxonomy node together with the permissible atomic-action vocabulary and returns a sequence of segments, each with an action label and precise start and end times. We gate all labels through the Subcategory vocabulary with synonym resolution, merge gaps and very short fragments to stabilize boundaries, and clamp timestamps to the clip duration. This produces atomic action spans aligned with human intent, surpassing the quality of uniform or fixed-length slicing.

3.4. Motion Estimation and Descriptions

Upon identifying an atomic-action segment, the clip is processed through two concurrent modules.

The first module estimates 3D human motion using GVHMR [71], producing outputs in the SMPL [46] body model format, which include global translation, root orientation, and 24 joint angles. These motion sequences are then resampled to 30FPS, standardized in body scale, and

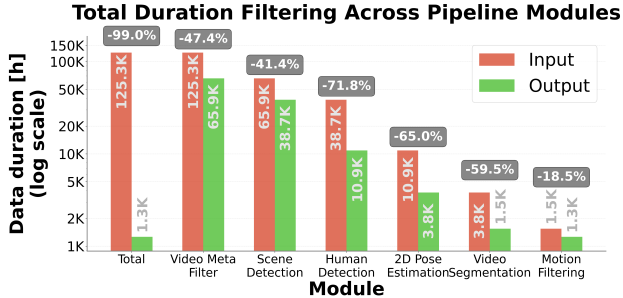


Figure 3. **Aggressive filtering.** Filtering out 99% of total input duration in our data pipeline. The chart shows the input (red) and output (green) hours for each filtering module, demonstrating a reduction from 125.3K to 1.3K total hours.

Motion Sequence Count by Data Source

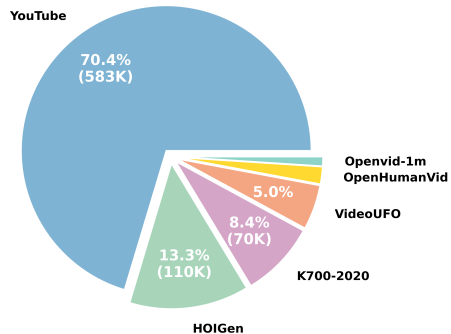


Figure 4. **Data source distribution for RoMo.** The pie chart illustrates the percentage breakdown of motion sequences sourced from web videos

orientation-aligned to ensure cross-instance comparability.

Simultaneously, the second module extracts text descriptions by utilizing Qwen3-VL [93] to generate K natural language descriptions for the motion sequence. Following this, these outputs undergo an additional processing stage, again using Qwen3-VL, to extract structured taxonomy labels (category, subcategory, and atomic action). This final step ensures that the extracted labels align with the provided taxonomy for inputs that have one, and generates new, consistent labels for those that do not (from video datasets).

3.5. Motion Evaluation and Filtering

When extracting motion from web videos, analyzing the motion’s level of dynamics has been grossly overlooked, a gap that, as we show, has resulted in datasets dominated by static or low-activity motions. To address this, we propose the *Dynamic Score*. The dynamic score quantifies motion activity by combining temporal and spatial characteristics.

Given a motion sequence with joint positions $\mathbf{P} \in \mathbb{R}^{F \times J \times 3}$ and joint velocities $\mathbf{V} \in \mathbb{R}^{F \times J \times 3}$ where F is the number of frames and J is the number of joints, we com-

pute two components. The *temporal component* measures instantaneous motion activity through velocity magnitudes:

$$S_{\text{temporal}} = \frac{1}{F \cdot J} \sum_{t=1}^F \sum_{j=1}^J \|\mathbf{v}_{t,j}\|_2 \quad (1)$$

The *spatial component* captures the overall extent of motion by measuring the range of each joint’s trajectory:

$$S_{\text{spatial}} = \frac{1}{J} \sum_{j=1}^J \left\| \max_t \mathbf{p}_{t,j} - \min_t \mathbf{p}_{t,j} \right\|_2 \quad (2)$$

These components are combined using weights w_v and w_r to produce the final dynamic score:

$$S_{\text{Dynamic}} = w_v \cdot S_{\text{temporal}} + w_r \cdot S_{\text{spatial}} \quad (3)$$

This hybrid approach ensures that both highly dynamic motions (e.g., dance, sports) and motions with large spatial coverage (e.g., reaching, walking) receive appropriate scores. Throughout the paper we use $(w_v, w_r) = (0.7, 0.3)$.

The dynamic score serves as our last-stage filter, allowing us to exclude motions that lack meaningful activity. Since different types of actions have inherently different dynamism levels (for example, gymnastics compared to screwing in a light bulb), we suggest an *adaptive per-category filtering* rather than a universal threshold. Selecting the top-P percentile within each category guarantees that even subtle activities remain well represented, while overly static clips are removed.

4. The RoMo Dataset

RoMo is an extensive 3D human motion dataset, sourced from a diverse collection of web videos and existing open-source datasets. It comprises 813,938 motion sequences that total $\sim 1,238$ hours of human motion at 30FPS. The clips have an average length of 165 frames (median 114), with all sequences capped to a duration between 30 and 600 frames. Each sequence is accompanied by five text descriptions and our taxonomy category, subcategory, and atomic action labels (see Fig. 4 for the data source distribution). As demonstrated in Tab. 1, RoMo is uniquely characterized by its hierarchical semantic taxonomy—a feature absent in existing datasets. While achieving a scale competitive with modern video-based collections, it far surpasses the diversity of traditional mocap data. Note that to ensure a fair comparison, we distinguish between the ‘total set’ (all reported sequences) and the ‘core set’ (newly introduced sequences). This separation is crucial because common practice often involves merging previous datasets, which obscures the actual number of novel motions contributed by a specific paper.

By organizing our data using this proposed taxonomy, we identify 54 categories and 2,065 distinct subcategories.

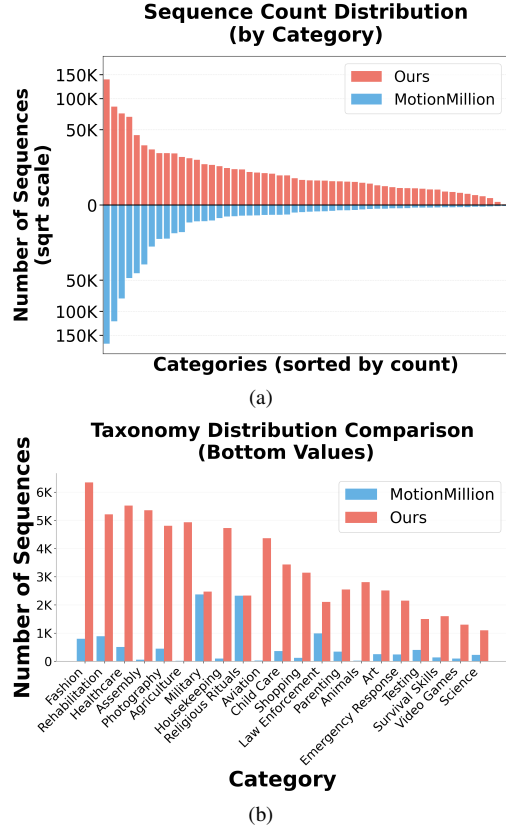


Figure 5. **Superior diversity and coverage.** Comparison of sequence counts per category between our RoMo and MotionMillion (a). The bottom figure (b) shows the “tail” of the distribution of both datasets on the same plot, demonstrating how our dataset provides better coverage of these less frequent categories.

When mapped to the same taxonomy, MotionMillion covers only 1,277 subcategories, marking a 61.7% increase in coverage for our dataset. Fig. 5 illustrates this superior diversity by comparing our sequence distribution against MotionMillion’s core set across all categories (a) and least common categories (b). For a comprehensive analysis at the subcategory level, please refer to the interactive HTML in the supplemental material.

Dynamic Score. A key contribution of our work is recognizing that motion datasets have long overlooked the distribution of motion dynamics, leading to inflated counts dominated by low-activity clips. Our analysis reveals a significant portion of moderate-to-low dynamic motions in existing data. For instance, when filtering the 559K sequences from the MotionMillion dataset by dynamic score thresholds ≥ 0.05 , ≥ 0.10 , ≥ 0.15 , and ≥ 0.50 , only 88.41%, 78.46%, 69.07%, and 31.55% of sequences are retained, respectively. This highlights a heavy skew towards low-dynamic content.

In contrast, our dataset is demonstrably more dynamic,

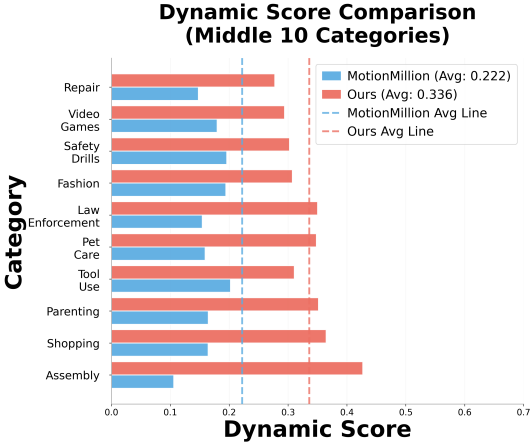


Figure 6. **Dynamic Score Analysis.** RoMo demonstrates higher dynamic scores across the majority of categories, with a 41% improvement in dynamic score. This figure shows a subset of 10 categories. (For all categories, see supplemental material.)

achieving a mean dynamic score of 0.336, which is 41.4% higher than MotionMillion’s 0.222. This per-category advantage is further detailed in Fig. 6, which illustrates that our dataset provides more dynamic motions across multiple categories. An extended per-category breakdown is provided in the supplemental material and reveals that categories inherently possess a broad range of dynamic scores (e.g., dance vs. eating), suggesting that models trained on such data must learn these differences implicitly.

Coverage and diversity. To assess the semantic coverage and diversity of RoMo, we performed a t-SNE analysis on its text captions (see Fig. 7). A qualitative comparison against MotionMillion and HumanML3D demonstrates that our dataset achieves better coverage and better diversity. Furthermore, we show internal semantic structure using our ‘Sports’ category, coloring each point by its subcategory (e.g., ‘swimming,’ ‘golf,’ ‘baseball’). The results reveal distinct, semantically meaningful clusters, which confirm that our dataset’s taxonomy successfully captures the hierarchical relationships between motions.

5. The Motion Toolbox

We introduce the Motion Toolbox, a Python library designed to standardize 3D human motion analysis and quality assessment. It provides a unified framework supporting multiple representations, including MotionMillion, HumanML3D, and various SMPL formats, with built-in converters for broad interoperability. The toolbox integrates research-validated metrics for physical plausibility—such as foot skating, ground penetration, jerk, and floating, proposed in prior works [55, 67, 80, 95]. Additionally, it features a web browser-based visualizer, enabling interactive inspection and rigorous evaluation of motion generation

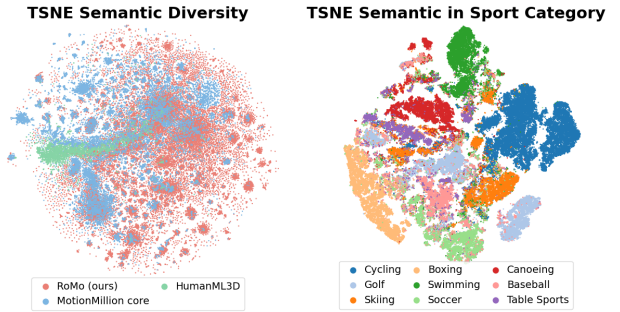


Figure 7. **t-SNE analysis.** (left) Comparison of RoMo (ours) and MotionMillion and HumanML3D, showing improved coverage. (right) Semantic clustering of ‘Sports’ category, where points are colored by subcategory, confirming our Taxonomy’s quality.

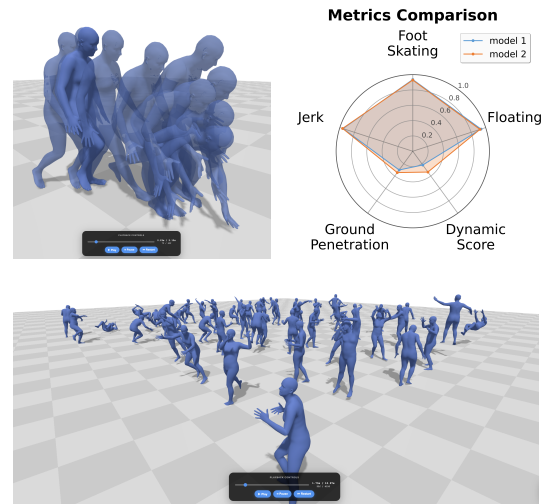


Figure 8. **Motion toolbox.** Our toolbox provides useful tools for visualizing keyframes (top left), a suite of evaluation metrics (top right) and an html multiple animations visualizer (bottom).

models. Fig. 8 Shows a subset of functionalities available in the toolbox, including the HTML motion visualizer and evaluation metric star chart. Please see HTML files in supplemental material to see the visualizer in action.

6. Experiments

Our evaluation framework follows standard practices in the field by assessing two key aspects of motion generation: (1) semantic alignment with the input text and (2) the physical fidelity of the resulting motion. For semantic alignment, we adopt Diversity, FID, Matching score, Dynamic score from prior work [22, 28, 79]. An evaluator was trained exclusively for text-motion alignment, based on the TMR [61] framework. This framework employs a reduced dimension that contains only root translation and rotation information as well as the joint rotations [22, 29]. Additionally, we eval-

Table 2. Motion generation performance for MDM (diffusion) and MMGPT (GPT) models on RoMo.

Method	Diversity \uparrow	FID \downarrow	Matching Score \uparrow	Dynamic Score \uparrow	Ground Penetration \downarrow ($\times 10^{-5}$)	Foot Skating \downarrow ($\times 10^{-3}$)	Floating \downarrow ($\times 10^{-2}$)
MDM	27.67	20.63	12.06	0.2138	0.0	1.70	1.67
MMGPT	16.68	12.80	22.08	0.3268	3.55	92.0	0.0311

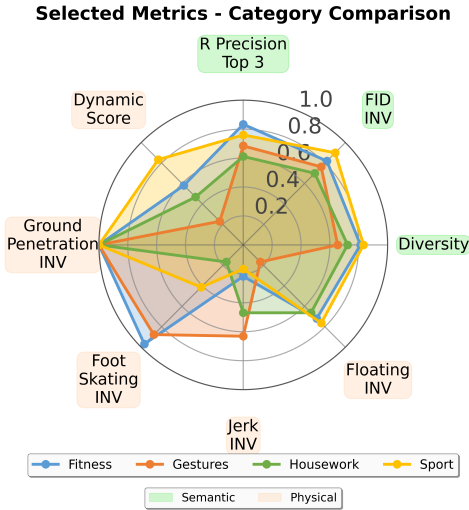


Figure 9. **Category wise evaluation of MDM [79] on RoMo.** We report the evaluation metrics on different categories and how the significant differences between them, highlighting the blind spots of the traditional aggregated reporting method. Some metrics were inverted (INV) to indicate higher-is-better.

uate physical fidelity. This is achieved by employing an established suite of physical metrics from our toolbox designed to detect common artifacts, including foot skating, ground penetration, floating, and jerk/jitter [34, 55, 67, 95].

Implementation details. We train two models on RoMo: MDM [79], a diffusion-based model and Motion-MillionGPT (MMGPT) [16] an autoregressive model. For MDM, a 50 diffusion step model was trained for 165k training steps using a transformer decoder architecture with a latent dimension of 512, feedforward size of 1024, 8 layers and 4 heads. We used an Adam Optimizer with a learning rate of $1e-4$ and batch size of 256. A BERT text encoder was used to encode text up to a maximum length of 128. The MDM model was trained to output 224 frame animations. This was trained on a single A100-80GB GPU.

For MMGPT we trained as described in their work [16] with default settings. The VAE was trained with a batch size of 2048, while the 3B Llama GPT model was trained with a batch size of 16. This model was trained on 4 A100-80GB GPUs, with 100k training iterations for the VAE and 75k

training iterations for the GPT model.

SOTA Model training. The results in Tab. 2 highlight a key architectural trade-off in motion generation. MMGPT, an autoregressive model, excels in FID and Matching Score. This suggests its token-based, sequential approach is highly effective at capturing the precise semantic mapping from text to motion (Matching Score) and modeling the fine-grained statistical properties of the real motion distribution (FID). Conversely, the diffusion-based MDM achieves superior Diversity and physical performance. Its denoising mechanism naturally produces a more varied set of motions for a single prompt. More importantly, its holistic, non-autoregressive refinement of the entire sequence appears to prevent the error accumulation common in sequential models, leading to motions with greater long-range consistency and physical plausibility. Interestingly, the GPT model achieved a mean dynamic score closer to the RoMo ground truth than MDM, highlighting its temporal effectiveness.

Taxonomy uncovers blind spots. We evaluate the performance of the MDM model on subcategories from our taxonomy and report the performance in Fig. 9. The results show that different categories portray vastly different performance in multiple metrics, highlighting the blind spots that exist when aggregated evaluation is performed.

7. Conclusions and Future Work

We introduced **RoMo** to address the critical lack of high-fidelity, large-scale human motion data. By employing adaptive filtering on in-the-wild sequences, our dataset successfully bridges the gap between constrained motion capture and noisy web collections. Beyond data, our novel **hierarchical taxonomy** transforms evaluation from opaque global metrics to transparent, per-category analysis.

Supported by the **Motion Toolbox** for standardized analysis, RoMo establishes a robust baseline for reproducible research and the next generation of truly generalizable human motion models. Our taxonomy-guided experiments demonstrate how fine-grained evaluation sheds new light on where generative models succeed and where they fall short, offering clarity that previous datasets could not provide. We encourage the community to leverage this framework to advance the next wave of high-fidelity, broadly capable human motion generation models.

References

- [1] Advanced Computing Center for the Arts and Design. AC-CAD MoCap Dataset. 3
- [2] Ijaz Akhter and Michael J. Black. Pose-conditioned joint angle limits for 3D human pose reconstruction. In *IEEE Conf. on Computer Vision and Pattern Recognition (CVPR) 2015*, 2015. 3
- [3] Simon Alexanderson, Rajmund Nagy, Jonas Beskow, and Gustav Eje Henter. Listen, denoise, action! audio-driven motion synthesis with diffusion models. *ACM Transactions on Graphics (TOG)*, 42(4):1–20, 2023. 2
- [4] Andreas Aristidou, Ariel Shamir, and Yiorgos Chrysanthou. Digital dance ethnography: Organizing large dance collections. *J. Comput. Cult. Herit.*, 12(4), 2019. 3
- [5] German Barquero, Sergio Escalera, and Cristina Palmero. Seamless human motion composition with blended positional encodings. In *Proceedings of the IEEE/CVF Conference on Computer Vision and Pattern Recognition*, pages 457–469, 2024. 3
- [6] Yizhak Ben-Shabat, Xin Yu, Fatemeh Saleh, Dylan Campbell, Cristian Rodriguez-Opazo, Hongdong Li, and Stephen Gould. The ikea asm dataset: Understanding people assembling furniture through actions, objects and pose. In *Proceedings of the IEEE/CVF Winter Conference on Applications of Computer Vision*, pages 847–859, 2021. 4
- [7] Federica Bogo, Javier Romero, Gerard Pons-Moll, and Michael J. Black. Dynamic FAUST: Registering human bodies in motion. In *IEEE Conf. on Computer Vision and Pattern Recognition (CVPR)*, 2017. 3
- [8] Samarth Brahmhatt, Cusuh Ham, Charles C. Kemp, and James Hays. ContactDB: Analyzing and predicting grasp contact via thermal imaging. In *The IEEE Conference on Computer Vision and Pattern Recognition (CVPR)*, 2019. 3
- [9] Fabian Caba Heilbron, Victor Escorcia, Bernard Ghanem, and Juan Carlos Niebles. Activitynet: A large-scale video benchmark for human activity understanding. In *Proceedings of the IEEE conference on computer vision and pattern recognition*, pages 961–970, 2015. 4
- [10] Carnegie Mellon University. CMU MoCap Dataset. 3
- [11] Joao Carreira and Andrew Zisserman. Quo vadis, action recognition? a new model and the kinetics dataset. In *proceedings of the IEEE Conference on Computer Vision and Pattern Recognition*, pages 6299–6308, 2017. 4
- [12] Anargyros Chatzitofis, Leonidas Saroglou, Prodrimos Boutis, Petros Drakoulis, Nikolaos Zioulis, Shishir Subramanyam, Bart Kevelham, Caecilia Charbonnier, Pablo Cesar, Dimitrios Zarpalas, et al. Human4d: A human-centric multimodal dataset for motions and immersive media. *IEEE Access*, 8:176241–176262, 2020. 3
- [13] Rui Chen, Mingyi Shi, Shaoli Huang, Ping Tan, Taku Komura, and Xuelin Chen. Taming diffusion probabilistic models for character control. In *ACM SIGGRAPH 2024 Conference Papers*, New York, NY, USA, 2024. Association for Computing Machinery. 2
- [14] Setareh Cohan, Guy Tevet, Daniele Reda, Xue Bin Peng, and Michiel van de Panne. Flexible motion in-betweening with diffusion models, 2024. 2
- [15] Rishabh Dabral, Muhammad Hamza Mughal, Vladislav Golyanik, and Christian Theobalt. Mofusion: A framework for denoising-diffusion-based motion synthesis. In *Proceedings of the IEEE/CVF Conference on Computer Vision and Pattern Recognition*, pages 9760–9770, 2023. 2
- [16] Ke Fan, Shunlin Lu, Minyue Dai, Runyi Yu, Lixing Xiao, Zhiyang Dou, Junting Dong, Lizhuang Ma, and Jingbo Wang. Go to zero: Towards zero-shot motion generation with million-scale data. In *Proceedings of the IEEE/CVF International Conference on Computer Vision*, pages 13336–13348, 2025. 2, 3, 5, 8
- [17] Nima Ghorbani and Michael J. Black. SOMA: Solving optical marker-based mocap automatically. In *Proc. International Conference on Computer Vision (ICCV)*, pages 11117–11126, 2021. 3
- [18] Saeed Ghorbani, Kimia Mahdavian, Anne Thaler, Konrad Kording, Douglas James Cook, Gunnar Blohm, and Nikolaus F. Troje. MoVi: A large multipurpose motion and video dataset. *arXiv preprint arXiv: 2003.01888*, 2020. 3
- [19] Aaron Grattafiori, Abhimanyu Dubey, Abhinav Jauhri, Abhinav Pandey, Abhishek Kadian, Ahmad Al-Dahle, Aiesha Letman, Akhil Mathur, Alan Schelten, Alex Vaughan, et al. The llama 3 herd of models. *arXiv preprint arXiv:2407.21783*, 2024. 2
- [20] Chuan Guo, Shihao Zou, Xinxin Zuo, Sen Wang, Wei Ji, Xingyu Li, and Li Cheng. Generating diverse and natural 3d human motions from text. In *Proceedings of the IEEE/CVF Conference on Computer Vision and Pattern Recognition (CVPR)*, pages 5152–5161, 2022. 3
- [21] Chuan Guo, Shihao Zou, Xinxin Zuo, Sen Wang, Wei Ji, Xingyu Li, and Li Cheng. Generating diverse and natural 3d human motions from text. In *Proceedings of the IEEE/CVF Conference on Computer Vision and Pattern Recognition*, pages 5152–5161, Washington, DC, USA, 2022. IEEE Computer Society. 2
- [22] Chuan Guo, Yuxuan Mu, Muhammad Gohar Javed, Sen Wang, and Li Cheng. Momask: Generative masked modeling of 3d human motions. In *Proceedings of the IEEE/CVF Conference on Computer Vision and Pattern Recognition*, pages 1900–1910, 2024. 2, 7
- [23] Fabian Helm, Nikolaus Troje, Mathias Reiser, and Jörn Munzert. Bewegungsanalyse getäuschter und nicht-getäuschter 7m-würfe im handball. 2015. 3
- [24] Martin Heusel, Hubert Ramsauer, Thomas Unterthiner, Bernhard Nessler, and Sepp Hochreiter. Gans trained by a two time-scale update rule converge to a local nash equilibrium. *Advances in neural information processing systems*, 30, 2017. 3
- [25] Jonathan Ho, Ajay Jain, and Pieter Abbeel. Denoising diffusion probabilistic models. *Advances in Neural Information Processing Systems*, 33:6840–6851, 2020. 2
- [26] Ludovic Hoyet, Kenneth Ryall, Rachel McDonnell, and Carol O’Sullivan. Sleight of hand: Perception of finger motion from reduced marker sets. In *Proceedings of the ACM SIGGRAPH Symposium on Interactive 3D Graphics and Games*, pages 79–86, 2012. 3
- [27] Yinghao Huang, Manuel Kaufmann, Emre Aksan, Michael J. Black, Otmar Hilliges, and Gerard Pons-Moll. Deep inertial

- poser learning to reconstruct human pose from sparse inertial measurements in real time. *ACM Transactions on Graphics, (Proc. SIGGRAPH Asia)*, 37(6):185:1–185:15, 2018. 3
- [28] Yiheng Huang, Hui Yang, Chuanchen Luo, Yuxi Wang, Shibiao Xu, Zhaoxiang Zhang, Man Zhang, and Junran Peng. Stablemofusion: Towards robust and efficient diffusion-based motion generation framework. In *Proceedings of the 32nd ACM International Conference on Multimedia*, pages 224–232, 2024. 7
- [29] Inwoo Hwang, Jian Wang, Bing Zhou, et al. Snapmogen: Human motion generation from expressive texts. In *The Thirty-ninth Annual Conference on Neural Information Processing Systems*. 3, 7
- [30] Catalin Ionescu, Dragos Papava, Vlad Olaru, and Cristian Sminchisescu. Human3.6m: Large scale datasets and predictive methods for 3d human sensing in natural environments. *IEEE transactions on pattern analysis and machine intelligence*, 36(7):1325–1339, 2013. 3
- [31] Biao Jiang, Xin Chen, Wen Liu, Jingyi Yu, Gang Yu, and Tao Chen. Motiongpt: Human motion as a foreign language. *Advances in Neural Information Processing Systems*, 36, 2024. 2
- [32] Glenn Jocher, Ayush Chaurasia, and Jing Qiu. Ultralytics yolov8, 2023. 5
- [33] Hanbyul Joo, Hao Liu, Lei Tan, Lin Gui, Bart Nabbe, Iain Matthews, Takeo Kanade, Shohei Nobuhara, and Yaser Sheikh. Panoptic studio: A massively multiview system for social motion capture. In *Proceedings of the IEEE international conference on computer vision*, pages 3334–3342, 2015. 3
- [34] Korrawe Karunratanakul, Konpat Preechakul, Supasorn Suwajanakorn, and Siyu Tang. Gmd: Controllable human motion synthesis via guided diffusion models. *arXiv preprint arXiv:2305.12577*, 2023. 2, 3, 8
- [35] Korrawe Karunratanakul, Konpat Preechakul, Emre Aksan, Thabo Beeler, Supasorn Suwajanakorn, and Siyu Tang. Optimizing diffusion noise can serve as universal motion priors. In *Proceedings of the IEEE/CVF Conference on Computer Vision and Pattern Recognition*, pages 1334–1345, 2024. 2
- [36] Franziska Krebs, Andre Meixner, Isabel Patzer, and Tamim Asfour. The KIT bimanual manipulation dataset. In *IEEE/RAS International Conference on Humanoid Robots (Humanoids)*, pages 499–506, 2021. 3
- [37] Black Forest Labs. Flux. <https://github.com/black-forest-labs/flux>, 2024. 2
- [38] Hsin-Ying Lee, Xiaodong Yang, Ming-Yu Liu, Ting-Chun Wang, Yu-Ding Lu, Ming-Hsuan Yang, and Jan Kautz. Dancing to music. *Advances in neural information processing systems*, 32, 2019. 2
- [39] Hui Li, Mingwang Xu, Yun Zhan, Shan Mu, Jiaye Li, Kaihui Cheng, Yuxuan Chen, Tan Chen, Mao Ye, Jingdong Wang, et al. Openhumanvid: A large-scale high-quality dataset for enhancing human-centric video generation. In *Proceedings of the Computer Vision and Pattern Recognition Conference*, pages 7752–7762, 2025. 4
- [40] Jiaman Li, Jiajun Wu, and C Karen Liu. Object motion guided human motion synthesis. *ACM Transactions on Graphics (TOG)*, 42(6):1–11, 2023. 2, 3
- [41] Quanzhou Li, Jingbo Wang, Chen Change Loy, and Bo Dai. Task-oriented human-object interactions generation with implicit neural representations. In *Proceedings of the IEEE/CVF Winter Conference on Applications of Computer Vision*, pages 3035–3044, 2024. 2
- [42] Yunzhi Li, Vimal Mollyn, Kuang Yuan, and Patrick Carrington. Wheelposer: Sparse-imu based body pose estimation for wheelchair users. In *Proceedings of the 26th International ACM SIGACCESS Conference on Computers and Accessibility*, pages 1–17, 2024. 3
- [43] Han Liang, Wenqian Zhang, Wenxuan Li, Jingyi Yu, and Lan Xu. Intergen: Diffusion-based multi-human motion generation under complex interactions. In *International Journal of Computer Vision*, pages 1–21, Berlin/Heidelberg, Germany, 2024. Springer. 2
- [44] Jing Lin, Ailing Zeng, Shunlin Lu, Yuanhao Cai, Ruimao Zhang, Haoqian Wang, and Lei Zhang. Motion-x: A large-scale 3d expressive whole-body human motion dataset. *Advances in Neural Information Processing Systems*, 36: 25268–25280, 2023. 3
- [45] Kun Liu, Qi Liu, Xinchen Liu, Jie Li, Yongdong Zhang, Jiebo Luo, Xiaodong He, and Wu Liu. Hoigen-1m: A large-scale dataset for human-object interaction video generation. In *Proceedings of the Computer Vision and Pattern Recognition Conference*, pages 24001–24010, 2025. 4
- [46] Matthew Loper, Naureen Mahmood, Javier Romero, Gerard Pons-Moll, and Michael J. Black. SMPL: A skinned multi-person linear model. *ACM Trans. Graphics (Proc. SIGGRAPH Asia)*, 34(6):248:1–248:16, 2015. 3, 5
- [47] Matthew M. Loper, Naureen Mahmood, and Michael J. Black. MoSh: Motion and shape capture from sparse markers. *ACM Transactions on Graphics, (Proc. SIGGRAPH Asia)*, 33(6):220:1–220:13, 2014. 3
- [48] Eyes JAPAN Co. Ltd. Eyes Japan MoCap Dataset. 3
- [49] Jiaxin Lu, Chun-Hao Paul Huang, Uttaran Bhattacharya, Qixing Huang, and Yi Zhou. Humoto: A 4d dataset of mocap human object interactions. In *Proceedings of the IEEE/CVF International Conference on Computer Vision (ICCV)*, pages 10886–10897, 2025. 3
- [50] Naureen Mahmood, N. Ghorbani, N. Troje, Gerard Pons-Moll, and Michael J. Black. Amass: Archive of motion capture as surface shapes. *2019 IEEE/CVF International Conference on Computer Vision (ICCV)*, pages 5441–5450, 2019. 3
- [51] Christian Mandery, Ömer Terlemez, Martin Do, Nikolaus Vahrenkamp, and Tamim Asfour. The KIT whole-body human motion database. In *International Conference on Advanced Robotics (ICAR)*, pages 329–336, 2015. 3
- [52] Christian Mandery, Ömer Terlemez, Martin Do, Nikolaus Vahrenkamp, and Tamim Asfour. The kit whole-body human motion database. In *2015 International Conference on Advanced Robotics (ICAR)*, pages 329–336. IEEE, 2015. 3
- [53] Christian Mandery, Ömer Terlemez, Martin Do, Nikolaus Vahrenkamp, and Tamim Asfour. Unifying representations and large-scale whole-body motion databases for studying human motion. *IEEE Transactions on Robotics*, 32(4):796–809, 2016. 3

- [54] Zichong Meng, Yiming Xie, Xiaogang Peng, Zeyu Han, and Huaizu Jiang. Rethinking diffusion for text-driven human motion generation. *arXiv preprint arXiv:2411.16575*, 2024. 2
- [55] Yuxuan Mu, Hung Yu Ling, Yi Shi, Ismael Baira Ojeda, Pengcheng Xi, Chang Shu, Fabio Zinno, and Xue Bin Peng. Stablemotion: Training motion cleanup models with unpaired corrupted data. *arXiv preprint arXiv:2505.03154*, 2025. 3, 7, 8
- [56] Lea Muller, Ahmed AA Osman, Siyu Tang, Chun-Hao P Huang, and Michael J Black. On self-contact and human pose. In *Proceedings of the IEEE/CVF Conference on Computer Vision and Pattern Recognition*, pages 9990–9999, 2021. 3
- [57] M. Müller, T. Röder, M. Clausen, B. Eberhardt, B. Krüger, and A. Weber. Documentation mocap database hdm05. Technical Report CG-2007-2, Universität Bonn, 2007. 3
- [58] Kepan Nan, Rui Xie, Penghao Zhou, Tieshan Fan, Zhenheng Yang, Zhijie Chen, Xiang Li, Jian Yang, and Ying Tai. Openvid-1m: A large-scale high-quality dataset for text-to-video generation. *arXiv preprint arXiv:2407.02371*, 2024. 4
- [59] Xiaogang Peng, Yiming Xie, Zizhao Wu, Varun Jampani, Deqing Sun, and Huaizu Jiang. Hoi-diff: Text-driven synthesis of 3d human-object interactions using diffusion models. *arXiv preprint arXiv:2312.06553*, 2023. 2
- [60] Mathis Petrovich, Michael J. Black, and Gül Varol. Action-conditioned 3D human motion synthesis with transformer VAE. In *International Conference on Computer Vision (ICCV)*, pages 10985–10995, Washington, DC, USA, 2021. IEEE Computer Society. 2
- [61] Mathis Petrovich, Michael J Black, and Gül Varol. Tmr: Text-to-motion retrieval using contrastive 3d human motion synthesis. In *Proceedings of the IEEE/CVF International Conference on Computer Vision*, pages 9488–9497, 2023. 7
- [62] Huaijin Pi, Zhi Cen, Zhiyang Dou, and Taku Komura. Coda: Coordinated diffusion noise optimization for whole-body manipulation of articulated objects. *arXiv preprint arXiv:2505.21437*, 2025. 2
- [63] Matthias Plappert, Christian Mandery, and Tamim Asfour. The kit motion-language dataset. *Big data*, 4(4):236–252, 2016. 3
- [64] Abhinanda R Punnakkal, Arjun Chandrasekaran, Nikos Athanasiou, Alejandra Quiros-Ramirez, and Michael J Black. Babel: Bodies, action and behavior with english labels. In *Proceedings of the IEEE/CVF conference on computer vision and pattern recognition*, pages 722–731, 2021. 3
- [65] Sigal Raab, Inbar Gat, Nathan Sala, Guy Tevet, Rotem Shalev-Arkushin, Ohad Fried, Amit H Bermano, and Daniel Cohen-Or. Monkey see, monkey do: Harnessing self-attention in motion diffusion for zero-shot motion transfer. *arXiv preprint arXiv:2406.06508*, 2024. 2
- [66] Alec Radford, Jeff Wu, Rewon Child, David Luan, Dario Amodei, and Ilya Sutskever. Language models are unsupervised multitask learners. 2019. 2
- [67] Roey Ron, Guy Tevet, Haim Sawdayee, and Amit H Bermano. Hoidini: Human-object interaction through diffusion noise optimization. *arXiv preprint arXiv:2506.15625*, 2025. 2, 3, 7, 8
- [68] Haim Sawdayee, Chuan Guo, Guy Tevet, Bing Zhou, Jian Wang, and Amit H Bermano. Dance like a chicken: Low-rank stylization for human motion diffusion. *arXiv preprint arXiv:2503.19557*, 2025. 2
- [69] Christoph Schuhmann, Richard Vencu, Romain Beaumont, Robert Kaczmarczyk, Clayton Mullis, Aarush Katta, Theo Coombes, Jenia Jitsev, and Aran Komatsuzaki. Laion-400m: Open dataset of clip-filtered 400 million image-text pairs. *arXiv preprint arXiv:2111.02114*, 2021. 3
- [70] Yoni Shafir, Guy Tevet, Roy Kapon, and Amit Haim Bermano. Human motion diffusion as a generative prior. In *The Twelfth International Conference on Learning Representations*, 2024. 2
- [71] Zehong Shen, Huaijin Pi, Yan Xia, Zhi Cen, Sida Peng, Zechen Hu, Hujun Bao, Ruizhen Hu, and Xiaowei Zhou. World-grounded human motion recovery via gravity-view coordinates. In *SIGGRAPH Asia Conference Proceedings*, 2024. 2, 3, 5
- [72] Soyong Shin, Juyong Kim, Eni Halilaj, and Michael J Black. Wham: Reconstructing world-grounded humans with accurate 3d motion. In *Proceedings of the IEEE/CVF Conference on Computer Vision and Pattern Recognition*, pages 2070–2080, 2024. 3
- [73] L. Sigal, A. Balan, and M. J. Black. HumanEva: Synchronized video and motion capture dataset and baseline algorithm for evaluation of articulated human motion. *International Journal of Computer Vision*, 87(1):4–27, 2010. 3
- [74] Li Siyao, Weijiang Yu, Tianpei Gu, Chunze Lin, Quan Wang, Chen Qian, Chen Change Loy, and Ziwei Liu. Bailando: 3d dance generation by actor-critic gpt with choreographic memory. In *Proceedings of the IEEE/CVF Conference on Computer Vision and Pattern Recognition*, pages 11050–11059, 2022. 2
- [75] Omid Taheri, Nima Ghorbani, Michael J. Black, and Dimitrios Tzionas. GRAB: A dataset of whole-body human grasping of objects. In *European Conference on Computer Vision (ECCV)*, 2020. 3
- [76] Omid Taheri, Nima Ghorbani, Michael J Black, and Dimitrios Tzionas. Grab: A dataset of whole-body human grasping of objects. In *Computer Vision—ECCV 2020: 16th European Conference, Glasgow, UK, August 23–28, 2020, Proceedings, Part IV 16*, pages 581–600. Springer, 2020. 3
- [77] Yansong Tang, Dajun Ding, Yongming Rao, Yu Zheng, Danyang Zhang, Lili Zhao, Jiwen Lu, and Jie Zhou. Coin: A large-scale dataset for comprehensive instructional video analysis. In *Proceedings of the IEEE/CVF Conference on Computer Vision and Pattern Recognition*, pages 1207–1216, 2019. 4
- [78] Guy Tevet, Brian Gordon, Amir Hertz, Amit H Bermano, and Daniel Cohen-Or. Motionclip: Exposing human motion generation to clip space. In *Computer Vision—ECCV 2022: 17th European Conference, Tel Aviv, Israel, October 23–27, 2022, Proceedings, Part XXII*, pages 358–374,

- Berlin/Heidelberg, Germany, 2022. Springer, Springer International Publishing. 2
- [79] Guy Tevet, Sigal Raab, Brian Gordon, Yoni Shafir, Daniel Cohen-or, and Amit Haim Bermano. Human motion diffusion model. In *The Eleventh International Conference on Learning Representations*, 2023. 2, 7, 8
- [80] Guy Tevet, Sigal Raab, Setareh Cohan, Daniele Reda, Zhengyi Luo, Xue Bin Peng, Amit Haim Bermano, and Michiel van de Panne. CLoSD: Closing the loop between simulation and diffusion for multi-task character control. In *The Thirteenth International Conference on Learning Representations*, 2025. 2, 3, 7
- [81] Shashank Tripathi, Lea Müller, Chun-Hao P. Huang, Taheri Omid, Michael J. Black, and Dimitrios Tzionas. 3D human pose estimation via intuitive physics. In *Proceedings of the IEEE/CVF Conference on Computer Vision and Pattern Recognition (CVPR)*, 2023. 3
- [82] Nikolaus F. Troje. Decomposing biological motion: A framework for analysis and synthesis of human gait patterns. *Journal of Vision*, 2(5):2–2, 2002.
- [83] Matt Trumble, Andrew Gilbert, Charles Malleson, Adrian Hilton, and John Collomosse. Total Capture: 3d human pose estimation fusing video and inertial sensors. In *2017 British Machine Vision Conference (BMVC)*, 2017. 3
- [84] Jonathan Tseng, Rodrigo Castellon, and Karen Liu. Edge: Editable dance generation from music. In *Proceedings of the IEEE/CVF Conference on Computer Vision and Pattern Recognition*, pages 448–458, 2023. 2
- [85] Shuhei Tsuchida, Satoru Fukayama, Masahiro Hamasaki, and Masataka Goto. Aist dance video database: Multi-genre, multi-dancer, and multi-camera database for dance information processing. In *ISMIR*, page 6, 2019. 3
- [86] Simon Fraser University and National University of Singapore. SFU Motion Capture Database. 3
- [87] Aaron Van Den Oord, Oriol Vinyals, et al. Neural discrete representation learning. *Advances in neural information processing systems*, 30, 2017. 2
- [88] Ashish Vaswani, Noam Shazeer, Niki Parmar, Jakob Uszkoreit, Llion Jones, Aidan N Gomez, Łukasz Kaiser, and Illia Polosukhin. Attention is all you need. *Advances in neural information processing systems*, 30, 2017. 2
- [89] Team Wan, Ang Wang, Baole Ai, Bin Wen, Chaojie Mao, Chen-Wei Xie, Di Chen, Feiwu Yu, Haiming Zhao, Jianxiao Yang, Jianyuan Zeng, Jiayu Wang, Jingfeng Zhang, Jingren Zhou, Jinkai Wang, Jixuan Chen, Kai Zhu, Kang Zhao, Keyu Yan, Lianghua Huang, Mengyang Feng, Ningyi Zhang, Pandeng Li, Pingyu Wu, Ruihang Chu, Ruili Feng, Shiwei Zhang, Siyang Sun, Tao Fang, Tianxing Wang, Tianyi Gui, Tingyu Weng, Tong Shen, Wei Lin, Wei Wang, Wei Wang, Wenmeng Zhou, Wenten Wang, Wenting Shen, Wenyuan Yu, Xianzhong Shi, Xiaoming Huang, Xin Xu, Yan Kou, Yangyu Lv, Yifei Li, Yijing Liu, Yiming Wang, Yingya Zhang, Yitong Huang, Yong Li, You Wu, Yu Liu, Yulin Pan, Yun Zheng, Yuntao Hong, Yupeng Shi, Yutong Feng, Zeyinzi Jiang, Zhen Han, Zhi-Fan Wu, and Ziyu Liu. Wan: Open and advanced large-scale video generative models. *arXiv preprint arXiv:2503.20314*, 2025. 2
- [90] Wenhao Wang and Yi Yang. Videoufo: A million-scale user-focused dataset for text-to-video generation. *arXiv preprint arXiv:2503.01739*, 2025. 4
- [91] Ye Wang, Sipeng Zheng, Bin Cao, Qianshan Wei, Weishuai Zeng, Qin Jin, and Zongqing Lu. Scaling large motion models with million-level human motions. *arXiv preprint arXiv:2410.03311*, 2024. 3
- [92] Yufei Xu, Jing Zhang, Qiming Zhang, and Dacheng Tao. Vit-pose: Simple vision transformer baselines for human pose estimation. *Advances in Neural Information Processing Systems*, 35:38571–38584, 2022. 5
- [93] An Yang, Anfeng Li, Baosong Yang, Beichen Zhang, Binyuan Hui, Bo Zheng, Bowen Yu, Chang Gao, Chengen Huang, Chenxu Lv, Chujie Zheng, Dayiheng Liu, Fan Zhou, Fei Huang, Feng Hu, Hao Ge, Haoran Wei, Huan Lin, Jialong Tang, Jian Yang, Jianhong Tu, Jianwei Zhang, Jianxin Yang, Jiayi Yang, Jing Zhou, Jingren Zhou, Junyang Lin, Kai Dang, Keqin Bao, Kexin Yang, Le Yu, Lianghao Deng, Mei Li, Mingfeng Xue, Mingze Li, Pei Zhang, Peng Wang, Qin Zhu, Rui Men, Ruize Gao, Shixuan Liu, Shuang Luo, Tianhao Li, Tianyi Tang, Wenbiao Yin, Xingzhang Ren, Xinyu Wang, Xinyu Zhang, Xuancheng Ren, Yang Fan, Yang Su, Yichang Zhang, Yinger Zhang, Yu Wan, Yuqiong Liu, Zekun Wang, Zeyu Cui, Zhenru Zhang, Zhipeng Zhou, and Zihan Qiu. Qwen3 technical report. *arXiv preprint arXiv:2505.09388*, 2025. 5
- [94] Vickie Ye, Georgios Pavlakos, Jitendra Malik, and Angjoo Kanazawa. Decoupling human and camera motion from videos in the wild. In *Proceedings of the IEEE/CVF conference on computer vision and pattern recognition*, pages 21222–21232, 2023. 3
- [95] Ye Yuan, Jiaming Song, Umar Iqbal, Arash Vahdat, and Jan Kautz. Physdiff: Physics-guided human motion diffusion model. In *Proceedings of the IEEE/CVF International Conference on Computer Vision (ICCV)*, 2023. 3, 7, 8
- [96] Jianrong Zhang, Yangsong Zhang, Xiaodong Cun, Shaoli Huang, Yong Zhang, Hongwei Zhao, Hongtao Lu, and Xi Shen. T2m-gpt: Generating human motion from textual descriptions with discrete representations. In *Proceedings of the IEEE/CVF Conference on Computer Vision and Pattern Recognition (CVPR)*, Washington, DC, USA, 2023. IEEE Computer Society. 2
- [97] Wanyue Zhang, Rishabh Dabral, Vladislav Golyanik, Vasileios Choutas, Eduardo Alvarado, Thabo Beeler, Marc Habermann, and Christian Theobalt. Bimart: A unified approach for the synthesis of 3d bimanual interaction with articulated objects. *Proceedings of the IEEE/CVF Conference on Computer Vision and Pattern Recognition (CVPR)*, 2025. 2
- [98] Yuhong Zhang, Jing Lin, Ailing Zeng, Guanlin Wu, Shunlin Lu, Yurong Fu, Yuanhao Cai, Ruimao Zhang, Haoqian Wang, and Lei Zhang. Motion-x++: A large-scale multimodal 3d whole-body human motion dataset. *arXiv preprint arXiv:2501.05098*, 2025. 3
- [99] Lei Zhong, Yiming Xie, Varun Jampani, Deqing Sun, and Huaizu Jiang. Smoodi: Stylized motion diffusion model. In *ECCV*, 2024. 2

RoMo: A Large-Scale, Richly Organized Dataset and Semantic Taxonomy for Human Motion Generation Supplementary Material

Jiahao Zhang^{1,2} Joseph Liu² Young-Yoon Lee² Seonghyeon Moon²
Victor Zordan² Guy Tevet³ C. Karen Liu³ Stephen Gould¹
Oren Jacob² Haomiao Jiang² Mubbasir Kapadia^{2,4} Yizhak Ben-Shabat²
¹Australian National University ²Roblox ³Stanford University ⁴Rutgers University

¹{jiaho.zhang, stephen.gould}@anu.edu.au

²{josephliu, ylee, smoon, vbzordan, haomiaojiang, ojacob, mkapadia, ibenshabat}@roblox.com

³{guytevet, karenliu}@cs.stanford.edu

<https://davidzhang73.github.io/romo-website>

Abstract

*This supplementary material provides extensive quantitative and interactive support for the claims presented in our main paper. We strongly encourage readers to engage with the accompanying interactive website and video, which offer a full demo of the **Motion Toolbox**, a Mindmap visualization of the novel semantic taxonomy, 3D rendered visualizations of motion samples from each category, and detailed analysis plots of our adaptive filtering approach. This document extends the model evaluation to include **MoMask++** and **MDM+BERT**, leveraging the taxonomy for a fine-grained, category-based analysis that reveals architecture-specific trade-offs. Furthermore, we present an ablation study quantifying the optimal trade-off in motion dynamics using our Dynamic Score ($S_{Dynamic}$), demonstrating that a refined subset (V_C) significantly improves generative performance (FID of 17.97 vs. 20.63 for the full set). Finally, we provide full implementation details for reproducibility and demonstrate the power of our hierarchical taxonomy with the **Context-Aware Adaptive Filtering methodology**, which strategically preserves authentic, category-specific motions while eliminating quality artifacts.*

1. Taxonomy-Based Fine-Grained Evaluation

Building upon the comparison of diffusion-based and GPT architectures in the main paper (Sec. 6), we extend our evaluation to include **MoMask++** [1] and **MDM+BERT** [2]. We report the performance of these models in Tab. 3 and Tab. 4 for semantic and physical metrics, respectively. Leveraging RoMo’s broad taxonomy allows for a fine-grained analysis that surfaces intriguing trade-offs between these architectures. For example, while MDM demonstrates

strong physical fidelity, MoMask++ achieves higher performance on semantic metrics, particularly FID (Fréchet Inception Distance), suggesting it better captures the statistical properties of the true motion distribution.

1.1. Taxonomy-Based Evaluation Insights

Our hierarchical taxonomy exposes a non-uniform model performance across motion categories, validating the need to move beyond aggregated metrics. For instance, MoMask++ significantly outperforms MDM in FID within categories characterized by subtle motions like *Communication*, *Education*, and *Gestures* (Tab. 5). To validate these variances, we evaluated 1,000 motion samples **randomly selected** per category across the top 10 most frequent categories. These results collectively suggest that diffusion-based approaches (MDM) offer better adherence to physical constraints, while transformer-based approaches (MoMask++) excel at capturing the distributional nuances of complex social and expressive motions.

1.2. Addressing Physical Quality Discrepancies

The performance disparities on physical metrics are pronounced (Tab. 6). MoMask++ shows significantly higher values for Jerk (e.g., 332.73 overall vs. 46.77 for MDM) and Acceleration Peaks, indicating less smooth and more artifact-prone sequences. This is typical for discrete tokenization approaches, where the quantization and sequential generation process can lead to accumulated temporal inconsistencies. Conversely, MDM’s holistic, non-autoregressive denoising mechanism appears to enforce superior long-range consistency and physical plausibility, leading to substantially smoother motion.

Dynamic Score Comparison
MotionMillion vs Ours

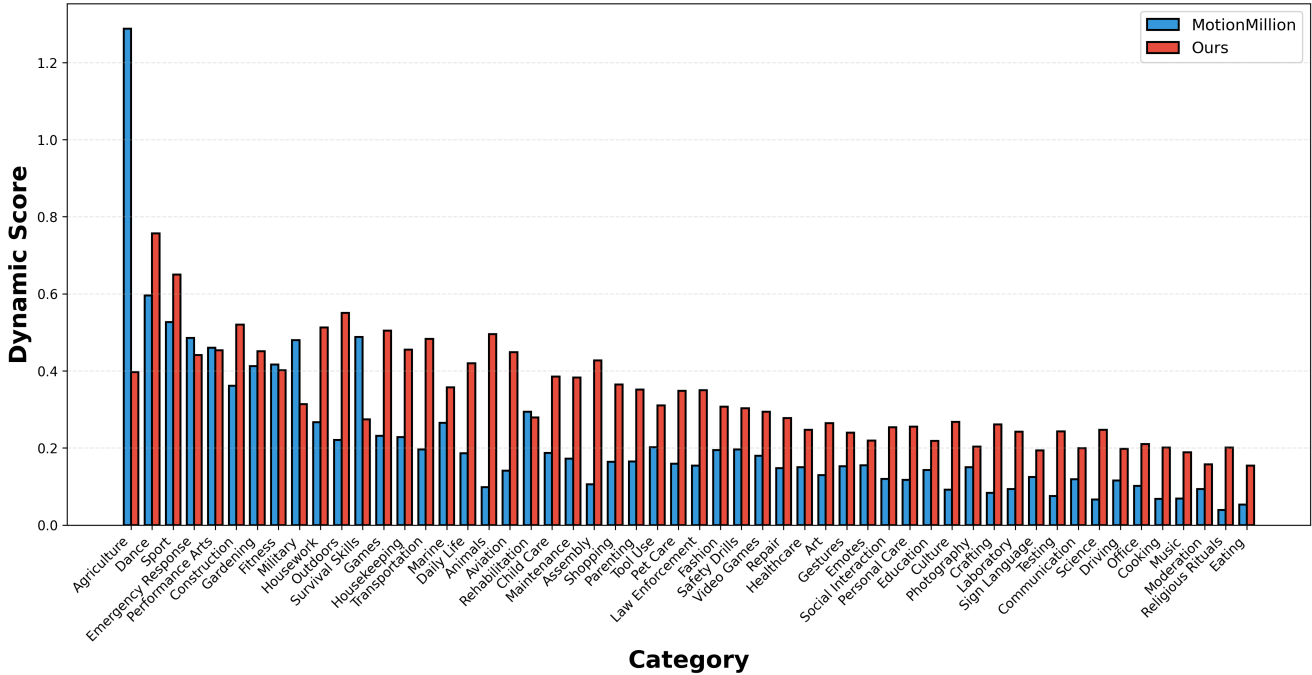


Figure 10. **Dynamic Score analysis.** RoMo demonstrates higher dynamic scores across the majority of categories

Table 3. **Semantic benchmark.** Comparison of text-to-motion generation quality between MoMask++ and MDM trained on the RoMo full dataset.

Method	R Precision			Diversity ↑	FID ↓	Matching Score ↑
	Top1	Top2	Top3			
MDM+BERT	0.5822	0.7578	0.8434	27.59	17.97	12.18
MoMask++	0.5148	0.6910	0.7820	28.17	14.30	12.86

2. Category-Wise Validation of Superior Motion Dynamics

Building on the global analysis provided in the main paper, we present a comprehensive per-category comparison of Dynamic Scores between our RoMo dataset and MotionMillion in Figure 10. This fine-grained breakdown substantiates our primary finding: RoMo consistently exhibits **higher motion intensity** across the vast majority of categories.

While MotionMillion may achieve higher Dynamic Scores in a few isolated categories, our dataset demonstrates a clear systematic advantage, validating that the substantial global increase in mean Dynamic Score (0.336 for RoMo vs. 0.222 for MotionMillion) is driven not by outliers, but by a systematic improvement in motion quality across the taxonomy. This per-category perspective is essential, as it confirms that RoMo provides a more reliable and vigorous

training signal across the entire spectrum of human activities.

3. Optimizing Training Signal via Dynamic Score Ablation

To quantify the impact of motion quality on generative performance, we conduct an ablation study across five mutually exclusive data partitions defined by our dynamic score ($S_{Dynamic}$). Starting from the complete dataset (A11), we define four distinct subsets (V_A, V_B, V_C, V_D) based on their dynamic range, testing MDM performance on each.

3.1. Dynamic Score Partitions

Starting from the full dataset (A11), we define four subsets by increasing the lower-bound threshold for inclusion: V_A ($S_{Dynamic} \geq 0.05$), V_B ($S_{Dynamic} \geq 0.1$), V_C ($S_{Dynamic} \geq 0.15$), and the highly-dynamic set V_D

Table 4. **Physical benchmark.** Comparison of physical motion artifacts and dynamic characteristics between MoMask++ and MDM.

Method	Foot Skating ↓	Jerk ↓	Ground Penetration ↓	Floating ↑	Acceleration Peaks ↑	Dynamic Score ↑
MDM+BERT	0.0011	46.77	0.00	0.0146	0.8374	0.2132
MoMask++	0.0022	332.73	2.1e−05	0.0020	4.7223	0.3887

Table 5. **Taxonomy-based semantic evaluation.** Fine-grained breakdown of generation quality comparing MDM and MoMask++ across the top 10 categories.

Category	Method	R Precision			Diversity ↑	FID ↓	Matching Score ↑
		Top1	Top2	Top3			
Overall	MDM	0.5822	0.7578	0.8434	27.59	17.97	12.18
	MoMask++	0.5148	0.6910	0.7820	28.17	14.30	12.86
Communication	MDM	0.3771	0.5363	0.6393	21.60	28.97	9.77
	MoMask++	0.3152	0.4635	0.5621	23.13	14.64	11.08
Daily Life	MDM	0.4782	0.6567	0.7537	26.55	27.80	12.15
	MoMask++	0.4066	0.5783	0.6760	26.56	21.27	12.91
Dance	MDM	0.3514	0.5111	0.6105	22.88	32.02	12.56
	MoMask++	0.3088	0.4459	0.5344	21.48	37.09	12.67
Education	MDM	0.3477	0.5221	0.6349	22.06	31.56	11.02
	MoMask++	0.3080	0.4641	0.5791	23.82	17.59	12.07
Fitness	MDM	0.5777	0.7525	0.8350	27.35	23.78	13.01
	MoMask++	0.5098	0.6895	0.7764	26.05	19.36	12.99
Gestures	MDM	0.4098	0.5723	0.6725	21.81	25.13	10.38
	MoMask++	0.3568	0.5125	0.6125	23.47	14.66	11.39
Housework	MDM	0.3431	0.5093	0.6107	24.38	27.58	12.98
	MoMask++	0.3139	0.4832	0.5900	23.40	24.69	12.96
Outdoors	MDM	0.4262	0.6125	0.7329	26.76	28.36	12.63
	MoMask++	0.3902	0.5689	0.6742	26.20	32.82	13.06
Pet Care	MDM	0.3807	0.5834	0.7004	24.72	33.23	11.56
	MoMask++	0.3018	0.4846	0.6096	24.90	30.54	12.56
Sport	MDM	0.4891	0.6820	0.7787	28.15	20.74	13.73
	MoMask++	0.4207	0.6158	0.7199	26.60	31.80	13.57

($S_{Dynamic} \geq 0.5$).

3.2. Semantic and Physical Insights

Results in Tab. 7 demonstrate that training on subset V_C yields the optimal semantic trade-off, achieving the best FID (17.97) compared to the full dataset (All, 20.63). This suggests that aggressively filtering sequences with lower dynamic scores effectively removes static noise that dilutes model performance.

However, training exclusively on the lowest dynamic range tested, V_D , results in a degraded FID (28.72) and significant physical instability (Jerk 113.35 in Tab. 8). This highlights that training solely on motion below the optimal dynamic threshold degrades motion smoothness and generation fidelity. It is important to note that while intermediate filtering (e.g., V_C) improves numerical metrics, highly aggressive filtering inevitably discards subtle, fine-grained interactions that are essential for a truly comprehensive and diverse motion distribution.

4. Context-Aware Adaptive Filtering

To demonstrate the unique utility of our hierarchical taxonomy, we present an adaptive filtering approach that takes advantage of category-specific semantic context to substantially improve the quality of the dataset while preserving critical motion diversity. We focus on the **foot skating ratio** metric—a measure of foot sliding artifacts common in motion capture data.

Traditional **global filtering** removes all samples with high foot skating values across the entire dataset. For instance, removing the top 15% of foot skating ratio samples results in 123,178 filtered samples. However, this indiscriminate approach fails to recognize that high foot skating values represent **authentic motion characteristics** in categories such as skateboarding, skiing, and snowboarding, while indicating quality issues in sedentary activities like office work or crafting.

Our adaptive filtering approach addresses this semantic

Table 6. **Taxonomy-based physical evaluation.** Fine-grained breakdown of physical motion quality and artifacts comparing MDM and MoMask++ across the top 10 categories.

Category	Method	Foot Skating ↓	Jerk ↓	Ground Penetration ↓	Floating ↑	Accel. Peaks ↑	Dynamic Score ↑
Overall	MDM	0.0011	46.77	0.0e+0	0.0146	0.8374	0.2132
	MoMask++	0.0022	332.73	2.1e−5	0.0020	4.7223	0.3887
Communication	MDM	0.0009	32.51	0.0e+0	0.0217	0.4239	0.0959
	MoMask++	0.0027	217.11	1.8e−6	0.0043	2.5882	0.2010
Daily Life	MDM	0.0036	49.18	0.0e+0	0.0054	1.0127	0.3941
	MoMask++	0.0019	320.67	5.1e−6	0.0010	4.6117	0.5264
Dance	MDM	0.0004	72.88	0.0e+0	0.0037	1.9088	0.3031
	MoMask++	0.0005	510.93	6.4e−6	0.0004	8.3472	0.5850
Education	MDM	0.0001	30.52	0.0e+0	0.0252	0.4201	0.1055
	MoMask++	0.0009	192.41	3.7e−7	0.0051	2.3672	0.1986
Fitness	MDM	0.0000	60.89	0.0e+0	0.0073	1.1000	0.2447
	MoMask++	0.0003	432.76	1.6e−8	0.0008	6.1700	0.4781
Gestures	MDM	0.0003	33.17	0.0e+0	0.0323	0.4644	0.1048
	MoMask++	0.0013	223.13	1.4e−6	0.0062	2.8128	0.2033
Housework	MDM	0.0029	40.42	0.0e+0	0.0121	0.7514	0.1924
	MoMask++	0.0023	345.09	1.4e−6	0.0013	5.6696	0.4160
Outdoors	MDM	0.0030	51.65	0.0e+0	0.0089	1.1816	0.4572
	MoMask++	0.0072	341.00	1.1e−5	0.0016	5.0046	0.5940
Pet Care	MDM	0.0100	51.41	1.0e−4	0.0188	0.8560	0.3216
	MoMask++	0.0225	306.83	9.3e−6	0.0027	3.9456	0.4358
Sport	MDM	0.0006	62.34	0.0e+0	0.0075	1.3625	0.3428
	MoMask++	0.0008	451.61	5.5e−6	0.0007	7.0758	0.6317

Table 7. **Ablation study on motion dynamics.** Evaluation of MDM performance across different data partitions defined by motion dynamic ($S_{Dynamic}$). The subsets range from high-dynamics (V_A) to low-dynamics (V_D). Results show that selective training (V_C) yields better semantic alignment (FID) than using the complete dataset (All).

Method	R Precision			Diversity ↑	FID ↓	Matching Score ↑
	Top1	Top2	Top3			
All	0.5893	0.7652	0.8441	27.67	20.63	12.06
VA	0.5754	0.7564	0.8473	27.66	19.61	12.18
VB	0.5863	0.7521	0.8414	27.82	18.70	12.24
VC	0.5822	0.7578	0.8434	27.59	17.97	12.18
VD	0.4660	0.6400	0.7441	28.79	28.72	14.26

ambiguity through the following steps:

1. **Category Identification:** We identify specific "expected skating" categories where foot skating is natural.
2. **Authenticity Preservation:** We preserve 100% of samples in these natural categories, regardless of their foot skating values.
3. **Contextual Filtering:** We apply **per-subcategory** 15% **filtering** to all other categories, removing only the worst samples relative to their specific contextual distribution.

This taxonomy-enabled methodology preserves **62, 733** high-quality authentic samples that would have been incorrectly removed by global filtering, while simultaneously identifying **45, 385** context-specific quality issues

that global filtering missed. This result demonstrates how our taxonomy provides the essential semantic structure needed to distinguish between authentic motion and quality artifacts, enabling a robust balance between quality improvement and diversity preservation.

The same adaptive filtering paradigm can be universally applied to other evaluation metrics:

- **Floating (vertical displacement):** Expected in jumping and acrobatic categories but signals errors elsewhere.
- **Ground Penetration:** Natural for digging and excavation activities but represents artifacts in most other contexts.

This flexibility demonstrates how the taxonomy enables researchers to design custom quality control pipelines tai-

Table 8. **Impact of motion dynamics on physical quality.** Physical metrics for MDM trained on different dynamic score subsets.

Method	Foot Skating ↓	Jerk ↓	Ground Penetration ↓	Floating ↑	Acceleration Peaks ↑	Dynamic Score ↑
All	1.70e-03	43.98	0.00e+00	0.0167	0.8171	0.2138
VA	9.61e-04	47.69	5.99e-06	0.0159	0.8859	0.2311
VB	1.57e-03	45.13	3.09e-05	0.0161	0.8558	0.2120
VC	1.10e-03	46.77	0.00e+00	0.0146	0.8374	0.2132
VD	4.23e-04	113.35	6.94e-04	2.85e-03	1.37	0.2711

lored to downstream tasks. We leave the exploration and evaluation of advanced adaptive filtering strategies within text-to-motion generation for future work.

5. Implementation Details

In the main paper we demonstrated the performance of several SOTA architectures (diffusion and GPT) when trained on our dataset. For reproducibility, we provide the implementation details for the different models.

MDM Training Parameters We train a Motion Diffusion Model using a transformer-based denoising architecture with 8 layers, 4 attention heads, latent dimension 512, and feedforward dimension 1024. Text conditioning is provided through a frozen BERT encoder with maximum sequence length of 128 tokens. The diffusion process employs 50 denoising steps during training. Motion sequences are processed with a maximum length of 224 frames at 30 FPS, corresponding to approximately 7.5 seconds of motion. We train with batch size 256 for 750,000 iterations using exponential moving average (EMA) of model weights without weight decay regularization.

MoMask++ Training Parameters We train MoMask++ on our ITW dataset, with adaptations for our hardware and dataset characteristics. In Stage 1, we train a hierarchical residual VQ-VAE with 6 quantizers across 4 scales (8, 4, 2, 1) using a codebook size of 512 and code dimension of 512. The encoder-decoder architecture uses a width of 512, depth of 3, and temporal downsampling factor of 2. We train for 1000 epochs with batch size 512, learning rate $3e-4$, and commitment loss weight 0.02. Critically, we disable gradient clipping to prevent codebook collapse, following recent findings in motion tokenization. In Stage 2, we train a bidirectional masked transformer with 8 layers, 6 attention heads, latent dimension 384, and feedforward dimension 1024. Text conditioning is provided via a frozen T5-base encoder (768-dim embeddings). We train for 500 epochs with batch size 256, applying linear learning rate scaling to $8e-4$ ($4\times$ the base rate of $2e-4$). Both stages use classifier-free guidance with 10% conditioning dropout and a 2000-step warmup schedule with multi-step learning rate decay at milestones [100k, 150k] with gamma 0.3. All experiments are conducted on a single NVIDIA A100-80GB GPU.

References

- [1] Inwoo Hwang, Jian Wang, Bing Zhou, et al. Snapmogen: Human motion generation from expressive texts. In *The Thirty-ninth Annual Conference on Neural Information Processing Systems*. 1
- [2] Guy Tevet, Sigal Raab, Brian Gordon, Yoni Shafir, Daniel Cohen-or, and Amit Haim Bermano. Human motion diffusion model. In *The Eleventh International Conference on Learning Representations*, 2023. 1